

## Mouse Kidney Progenitor Cells Accelerate Renal Regeneration and Prolong Survival After Ischemic Injury

PO-TSANG LEE,<sup>a,b</sup> HSI-HUI LIN,<sup>c</sup> SI-TSE JIANG,<sup>d</sup> PEI-JUNG LU,<sup>a</sup> KANG-JU CHOU,<sup>b</sup> HUA-CHANG FANG,<sup>b</sup> YUAN-YOW CHIOU,<sup>e</sup> MING-JER TANG<sup>c</sup>

<sup>a</sup>Institute of Clinical Medicine, College of Medicine, National Cheng Kung University, Tainan, Taiwan;

<sup>b</sup>Division of Nephrology, Department of Medicine, Kaohsiung Veterans General Hospital, Kaohsiung and National Yang-Ming University, School of Medicine, Taiwan; <sup>c</sup>Department of Physiology, College of Medicine, National Cheng Kung University, Tainan, Taiwan; <sup>d</sup>National Laboratory Animal Center, National Applied Research Laboratory, Taiwan; <sup>e</sup>Department of Pediatrics, National Cheng-Kung University Medical Center, Tainan, Taiwan

**Key Words.** Adult stem cell • Kidney • Acute renal failure • Cell therapy • Reperfusion injury

### ABSTRACT

Acute tubular necrosis is followed by regeneration of damaged renal tubular epithelial cells, and renal stem cells are supposed to contribute to this process. The purpose of our study is to test the hypothesis that renal stem cells isolated from adult mouse kidney accelerate renal regeneration via participation in the repair process. A unique population of cells exhibiting characteristics consistent with renal stem cells, mouse kidney progenitor cells (MKPC), was isolated from Myh9 targeted mutant mice. Features of these cells include (1) spindle-shaped morphology, (2) self-renewal of more than 100 passages without evidence of senescence, and (3) expression of Oct-4, Pax-2, Wnt-4, WT-1, vimentin,  $\alpha$ -smooth muscle actin, CD29, and S100A4 but no SSEA-1, c-kit, or other markers of more differentiated cells. MKPC exhibit plasticity as demonstrated by the

ability to differentiate into endothelial cells and osteoblasts in vitro and endothelial cells and tubular epithelial cells in vivo. The origin of the isolated MKPC was from the interstitium of medulla and papilla. Importantly, intrarenal injection of MKPC in mice with ischemic injury rescued renal damage, as manifested by decreases in peak serum urea nitrogen, the infarct zone, and the necrotic injury. Seven days after the injury, some MKPC formed vessels with red blood cells inside and some incorporated into renal tubules. In addition, MKPC treatment reduces the mortality in mice after ischemic injury. Our results indicate that MKPC represent a multipotent adult stem cell population, which may contribute to the renal repair and prolong survival after ischemic injury. *STEM CELLS* 2010;28:573–584

Disclosure of potential conflicts of interest is found at the end of this article.

### INTRODUCTION

Acute kidney injury is a potentially devastating problem in clinical medicine. After injury, the kidney undergoes a regenerative response that leads to recovery of renal function. However, kidney regeneration is frequently inadequate, resulting in significant morbidity and mortality [1]. Consequently, approximately 40% of patients fail to completely recover their renal function and discharge with residual renal failure [2, 3], and 10% of these patients require renal replacement therapy after 5 years [4]. Despite advances in the understanding of acute kidney injury and regeneration, therapeutic advances have been limited because of the complexity of kidney. Stem cell-based therapy is a new strategy in the treatment of acute

kidney injury and has potentially more value than single-agent drug therapy due to the highly versatile response of cells to their environment. These cells may not only secrete cytokines within the injured kidney but also participate in endothelial cell proliferation or angiogenesis to facilitate renal regeneration. In rodents, increasing evidence suggests that the therapeutic potential of mesenchymal stem cells derived from bone marrow could be beneficial in the kidney injury [5–8]. However, therapy with renal stem cells for kidney injury still awaits investigation.

Although studies have reported to isolate renal stem cells [9–14], the localization and the markers of renal stem cells remain controversial. The functional unit of the kidney is the nephron. Each human kidney contains  $0.6 \times 10^6$  to  $1.4 \times 10^6$  nephrons [15–17], which contrasts with the approximately

Author contributions: P.-T.L.: Conception and design, experimentation, data collection, data analysis and interpretation, and manuscript writing; H.-H.L.: Experimentation, data assembly, analysis, and interpretation, manuscript writing; P.-T.L. and H.-H.L. contributed equally to this work; S.-T.J.: Construction of tissue-specific expression of gene and provision of transgenic mice; P.-J.L.: Advice on experimental design, data analysis, and manuscript writing; K.-J.C.: Experimentation, data collection, and assistance of funding; Y.-Y.C.: Provision of study materials and instrumentation, help on collection of data; H.-C.F.: Experimentation and data collection; M.-J.T.: Supervision of the research direction, design and strategic approach, advice on data analysis and interpretation, and manuscript writing.

Correspondence: Ming-Jer Tang, M.D., Ph.D., Dept. of Physiology, College of Medicine, National Cheng Kung University, 1 Da-Hsueh Road, Tainan 701, Taiwan. Telephone: 886-6-235-3535, ext. 5425; Fax: 886-6-236-2780; e-mail: mjtang1@mail.ncku.edu.tw Received June 19, 2009; accepted for publication January 12, 2010; first published online in *STEM CELLS EXPRESS* January 22, 2010. © AlphaMed Press 1066-5099/2009/\$30.00/0 doi: 10.1002/stem.310

30,000 nephrons in each adult rat kidney [18]. The essential components of the nephron include the renal corpuscle (glomerulus and Bowman's capsule), the tubules, and the surrounding interstitium. Except for the collecting duct epithelia, which are derived from the ureteric bud, the metanephric mesenchyme forms tubular epithelial cells via mesenchymal-epithelial transition during kidney development [19, 20]. It has been shown that the metanephric mesenchyme contains renal stem cells [20, 21]. Considering the vulnerability of tubular cells to injuries through direct exposure to toxins in the tubular lumen, we hypothesize that renal interstitium may serve as a better niche for adult renal stem cells. The proximity of renal interstitium to renal tubules may also help to supply the damaged tubular cells in a short period of time.

There are few reports regarding the use of kidney stem cells in treating acute renal failure. Kidney stem cells in rats were isolated by Gupta et al. [12] using culture conditions that were similar to those used for the culture of bone marrow-derived multipotent adult progenitor cells. These cells can differentiate into renal tubules when injected intra-arterially after ischemia-reperfusion injury. No differences in renal function were observed between control group and stem cell-treated group. The aim of our study was to isolate and characterize a population of renal progenitor cells and to test whether these cells could participate in renal repair after acute kidney injury. To test our hypothesis, we used *Myh9* targeted mutant mice, in which a part of the stop codon of the last exon of *Myh9* is exchanged by GFP gene. *Myh9* encodes a non-muscle myosin heavy chain IIA [22, 23], which is mainly expressed in the cell cortex and stress fibers in non-muscle cells [23, 24]. The reason for choosing the *Myh9* locus to identify renal progenitor cell population is that *Myh9* protein is expressed in all interstitial cells. We report here the isolation of a unique population of cells, the mouse kidney progenitor cells (MKPC), that behave in a manner consistent with renal stem cells. Furthermore, intrarenal injection of these MKPC cells can rescue renal damage and prolong survival in severe combined immunodeficient (SCID) mice with renal ischemic injury.

## MATERIALS AND METHODS

### Generation of *Myh9* Targeted Mutant Mice and Breeding Scheme

A targeting plasmid was constructed using genomic DNA fragments derived from 129X1/SvJ mouse strain. A part of the last exon of *Myh9* containing 36 coding nucleotides before the stop codon and a 542 bp fragment following the stop codon were replaced by an emGFP coding sequence connecting with two bovine growth hormone poly A tails and an inverted *mc1* promoter-driven neomycin resistance gene flanked by two *loxP* sites. A 79 bp leading sequence of the last exon was preserved to link with emGFP coding sequence in-frame. The third *loxP* site was inserted into intron 40 of *Myh9*. A phosphoglycerate kinase promoter-driven thymidine kinase gene was used for negative selection. The targeting construct was then introduced into embryonic stem (ES) cell for homologous recombination by electroporation. The genomic DNA was isolated from neomycin and gancyclovir double-resistant ES cell clones and screened for a specific targeting event by polymerase chain reaction (PCR1 in Fig. 1A) using a forward primer in the *neo* sequence (5'-TGCTCCAAATGTGATGTGTCAGC-3') and a reverse primer outside the targeting vector (5'-TGCCCAGTCATAGCCGAATAGC-3'). To demonstrate the presence of the *loxP* in intron 40, one set of primers flanking the *loxP* site (forward; 5'-TTTGTT CCCAGCC-

CATCCTG-3' and backward; 5'-ACGAAATAAGTGGACCCAGAAAGC-3') was used (PCR2 in Fig. 1A). All the PCR products amplified from positive clones were confirmed by sequencing. The correct targeting of PCR positive clones was confirmed by Southern blot analysis. Blots were hybridized with digoxigenin-11-UTP (Roche, Basel, Switzerland, <http://www.roche-applied-science.com>)-labeled probe (Fig. 1B). DNA probes for Southern hybridization were cloned by PCR using the following primer set: 5'-CAGCCAGTGATAGCATCCAGA' (forward primer) and 5'-AGCAAGTGTCAGGATGTC-3' (backward primer). PCR DNA fragment (248 bp) were checked by 1.5% agarose gel electrophoresis and purified by Gel/PCR DNA fragments extraction kit (Geneaid Biotech Ltd., Taiwan, <http://www.geneaid.com/>, Cat. DF300). Three positive clones (clones 35, 161, and 405) were identified from 419 picked clones, and two independent clones (35 and 405) were injected into C57BL/6J blastocysts to generate chimeras. The chimeras were bred with C57BL/6J inbred strain mice to confirm germ-line transmission by PCR analysis and/or Southern blot. The heterozygotes were further backcrossed with C57BL/6J mice for five more generations (N6 progeny of congenic C57BL/6J), and homozygotes (N6F1 progeny) were generated by intercrossing between congenic heterozygotes (N6 progeny). Heterozygote and homozygote status were determined by Southern blot and PCR analysis of genomic DNA (Fig. 1B, 1C).

### Isolation of MKPC

All animal studies were approved by the Institutional Animal Care and Use Committee at Kaohsiung Veterans General Hospital. MKPC were isolated from the kidney of 2-month-old *Myh9* targeted mutant mice that contain a transgene of emGFP under the control of the mouse *Myh9* sequence. Kidneys were perfused in vivo with saline to flush out the blood from the kidney, dissected, minced, and digested with collagenase 0.3% and trypsin 0.3% at 37°C for 30 minutes in shaking water bath. After passing through 100  $\mu$ m mesh to remove undigested chunk, glomeruli, and large renal tubules, the filtered fraction was homogenized in a Dounce homogenizer for 10 strokes and then 40  $\mu$ m mesh was used to remove smaller renal tubules and cell aggregates. The filtered fraction containing mainly single cells was washed in a medium that consisted of Dulbecco's modified Eagle's medium (DMEM)-LG, 100 U/ml of penicillin, 100  $\mu$ g/ml of streptomycin, and 100  $\mu$ g/ml of gentamicin with 10% charcoal-stripped calf serum (CCS). Similar cell preparations from C57BL/6J mice were used to determine the level of autofluorescence. The cells prepared from *Myh9* targeted mutant mouse that express green fluorescence 10-fold higher than those from C57BL/6J mouse were sorted by fluorescence-activated cell sorting using FACSAria Cell Sorter (BD Biosciences, San Diego, <http://www.bdbiosciences.com>) equipped to sort green fluorescence protein (GFP). After sorting, GFP-positive cells were plated and cultured on plastic plates in LG-DMEM with 100 U/ml of penicillin, 100  $\mu$ g/ml of streptomycin, and 10% CCS (HyClone, Logan, UT, <http://www.hyclone.com>) at 37°C in the presence of 5% CO<sub>2</sub>.

### Characterization of MKPC

#### Immunocytochemistry of MKPC

MKPC cells, grown on collagen coated slides, were washed two times with phosphate-buffered saline (PBS) and fixed in 4% paraformaldehyde for 30 minutes. After being rinsed with PBS, cells were permeabilized with 0.1% Triton X-100 PBS for 15 minutes and then blocked in Superblock for 1 hour. Cells were then incubated with primary antibodies for 1 hour at room temperature in a moist box. The following primary antibodies were used: rabbit polyclonal anti-Pax 2 (Covance, Princeton, NJ, <http://www.covance.com>, PRB-276P, 1:400), rabbit polyclonal anti-Oct-4 (Chemicon, Temecula, CA, <http://www.chemicon.com>, MAB4305, 1:300), mouse monoclonal anti-SSEA-1 (Chemicon, MAB4301, 1:300), rat monoclonal anti-c-kit (Chemicon, CBK1360, 1:300),

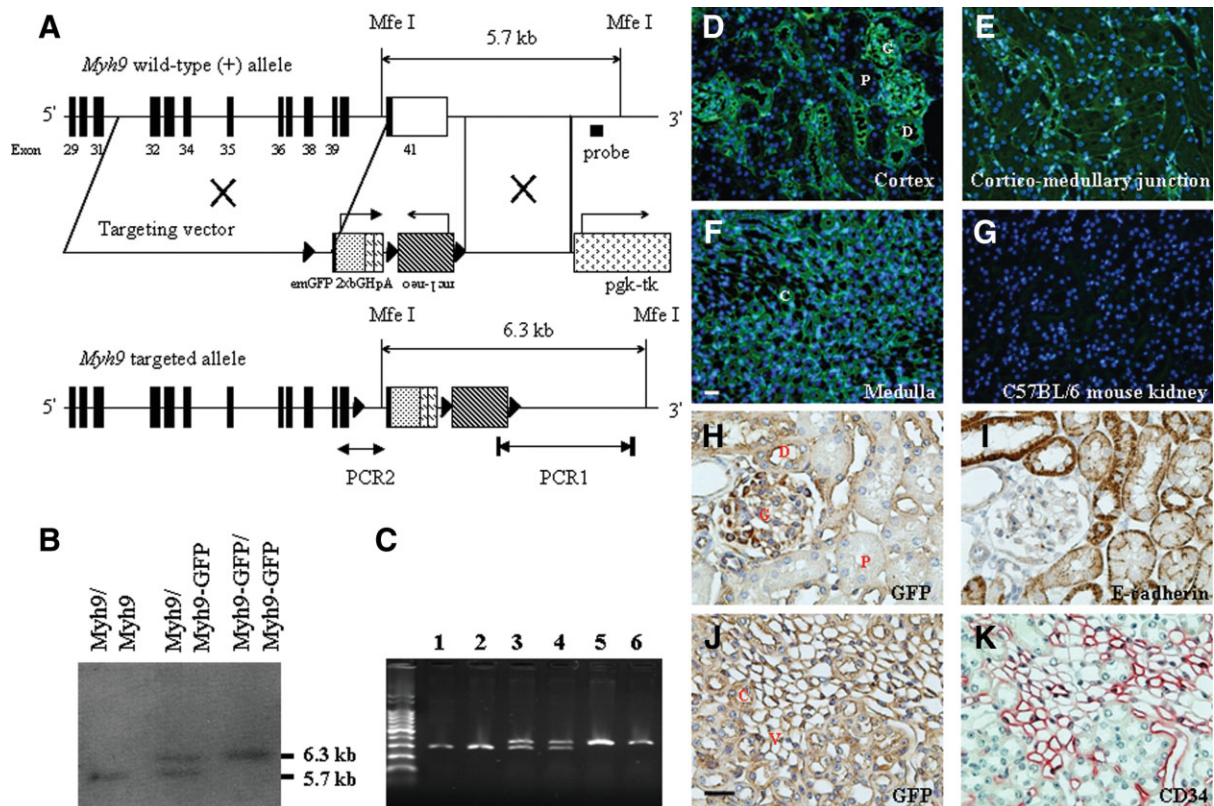


**Figure 1.** Targeting of the *Myh9* locus by homologous recombination and expression of emGFP tagged myosin heavy chain 9 in the kidney of targeted mutants. (A): Structure of wild-type and targeted *Myh9* alleles. The exons are numbered and depicted by filled boxes (coding region) or open box (noncoding region). The targeting vector was constructed as described in Materials and Methods. (B): Southern blot analyses of targeted mouse mutants. DNA isolated from F2 littermates derived from intercrossing of F1 heterozygotes was digested with Mfe I and hybridized with the probe outside the targeting alleles. The 5.7- and 6.3-kb bands represent wild-type (*Myh9*-GFP) alleles, respectively. (C): Reverse transcription PCR of the wild-type, heterozygous, and homozygous kidneys and tails using primer sets. Lanes are as follows: Lane 1, wide-type mouse kidney; lane 2, wide-type mouse tail; lane 3, heterozygous mouse kidney; lane 4, heterozygous mouse tail; lane 5, homozygous mouse kidney; lane 6, homozygous mouse tail. (D–G): Immunohistochemistry of kidney from *Myh9* targeted mutants. Green fluorescence protein (GFP) tagged myosin heavy chain 9 is expressed in the glomeruli, interstitium, and all tubules except only faintly in the brush border of proximal tubule. C57BL/6J mouse kidney was used as negative control. (H–K): Expression of GFP (H, J), E-cadherin (I), and CD 34 (K) in consecutive sections of the kidney. Distal tubules, collecting ducts, and peritubular capillaries expressed GFP. Scale bars: 50  $\mu$ m. Abbreviations: C, collecting duct; D, distal tubule; G, glomerulus; P, proximal tubule; PCR, polymerase chain reaction; V, vessel.

mouse monoclonal anti-E-cadherin antibody (BD 610181, 1:1000), mouse polyclonal anti-vimentin (Chemicon, MAB3400, 1:200), mouse monoclonal anti-alpha smooth muscle actin antibody (Sigma-Aldrich, St. Louis, <http://www.sigmaaldrich.com>, A2547, 1:800), rat anti- $\beta$ 1-integrin (R&D Systems Inc., Minneapolis, <http://www.rndsystems.com>, 1:500), and rabbit polyclonal anti-S100A4 (DakoCytomation, Glostrup, Denmark, <http://www.dakocytomation.com>, A5114, 1:200). Following three washes with tris-buffered saline (TBS), cells were incubated with Alexa 594-conjugated secondary antibodies (Molecular Probes Inc., Eugene, OR, <http://probes.invitrogen.com>) in PBS. Hoescht 33,258 was used for nuclear counterstaining. After washing, slides were mounted with a cover slip in Glycergel Antifade Medium (DAKO, Glostrup, Denmark, <http://www.dako.com>). Negative controls were performed using non-immune serum or IgG instead of the primary antibodies. Images were obtained using Olympus confocal fluorescence microscopy.

### Reverse Transcription PCR

Total RNA was extracted from MKPC or mMSC using Trizol Reagent (Invitrogen, Carlsbad, CA, <http://www.invitrogen.com>). Two  $\mu$ g of total RNA was reverse-transcribed into cDNA with

oligo-dT primer and MMLV reverse transcriptase (Invitrogen). PCR was performed with specific primer sets at 94°C for 30 seconds, 60°C for 30 seconds, and 72°C for 30 seconds (25 cycles) and followed by 72°C for 10 minutes. The forward and reverse primers were designed by Primer 3 for mouse gene: TCC CAG TGT CTC ATC CAT CA (forward primer) and GTT AGA GGC GCT GGA AAC AG (backward primer) for Pax-2, CAC GAG TGG AAA GCA ACT CA (forward primer) and AGA TGG TGG TCT GGC TGA AC (backward primer) for Oct-4, GAC TCA GTG AGC CCC ATC AT (forward primer) and AGA TCG TCT TGG CAG ATG CT (backward primer) for CD11b, ACC ACA GAC TTC CCC AAC TG (forward primer) and CGG ATT CCA GAG CAT TTG AT (backward primer) for CD34, CCA CCA GGG ACT GAC AAG TT (forward primer) and TGT AAT TTG TTT GGG CAC GA (backward primer) for CD45, CCA TCA ATT ACC TGC CCC TA (forward primer) and TTC CTG GCA ACA GGA AGT CT (backward primer) for Sca-1, ATT TTC TG GGC AGG AAG TT (forward primer) and ACG TCA GAA CAA CCG AAT CC (backward primer) for CD106, CGC TCT CCT GCT CTC AGT CT (forward primer) and GCA CGT GCT TCC TCT TCT CT (backward primer) for CD90, AGA ACT GGA GAA GTG TGG CTG TGA CC (forward primer) and TGT ATG TGG CTT GAA CTG TGC ATT CCG (backward

primer) for Wnt-4, ACA TCC GAC TTC CAA GAC AGC ACA C (forward primer) and TTG CAG CCA GAC CTC TGA AAT TCT G (backward primer) for WT-1, and ACG GCA CAT TCA AGG CTG AG (forward primer) and GGA GGC CAT GTA GAC CAT GAG G (backward primer) for glyceraldehyde-3-phosphate dehydrogenase. PCR products were subjected to 2% agarose gel electrophoresis, stained with ethidium bromide, and visualized under UV transilluminator.

### In Vitro Differentiation

For in vitro differentiation of cloned MKPC,  $10^5$  intact cells were plated onto 6 cm culture dish. Adipocyte differentiation was induced in DMEM culture medium containing 1-methyl-3-isobutylxanthine,  $10^{-9}$  M dexamethasone, 5 mM insulin, and 5 mM indomethacin (Stem Cell Technologies, Vancouver, BC, Canada, <http://www.stemcell.com>) and stained with saturated Oil-Red O solution (Sigma) in 60% isopropanol for detecting oil droplets 4 and 8 weeks later [25]. Endothelial differentiation was induced by growing MKPC in matrigel or human umbilical vein endothelial cells on matrigel-coated wells ( $15,000$  cells/ $m^2$ ) and was assessed by the specific morphology and the expression of von Willebrand factor by immunocytochemistry. Osteogenic differentiation was induced in DMEM culture medium containing  $50$   $\mu$ g/ml of ascorbic acid,  $10$  mM  $\beta$ -glycerophosphate, and  $10^{-9}$  M dexamethasone. Cell differentiation was tested 6 weeks later. For detection of calcium deposition, Alizarin red staining (Sigma) was used as described previously.

### Telomerase Activity

Telomeric repeat amplification protocol (TRAP) assay was performed using TeloTAGGG Telomerase PCR ELISA (Roche Diagnostics, Basel, Switzerland, <http://www.roche-applied-science.com>) to analyze relative telomerase activity (RTA) according to the protocol.  $2 \times 10^5$  cells per reaction were used. The absorbance of the samples was measured at 450 nm using an ELISA microtiter plate reader within 30 minutes after addition of the stop reagent.

### In Vivo Differentiation

The in vivo differentiation of MKPC was studied in normal kidneys. Six C57BL/6J mice were anesthetized with intraperitoneal injection of xylazine (3  $\mu$ g/g) and ketamine (150  $\mu$ g/g), and a volume of 100  $\mu$ l PBS containing  $10^5$  MKPC cells was slowly injected directly into the renal parenchyma of each kidney. The kidneys were harvested 30 days later to examine the in vivo differentiation of the injected cells. The mobilization of injected cells was traced by using fluorescence or anti-GFP antibody by immunohistochemistry.

### Effect of MKPC on Renal Rescue After Ischemia-Reperfusion Injury

To determine whether MKPC injection facilitated the recovery of renal function, 18 SCID mice ( $n = 6$  for each time point) were anesthetized with intraperitoneal injection of xylazine (3  $\mu$ g/g) and ketamine (150  $\mu$ g/g). Ischemic injury was operated by using flank incisions, and nontraumatic vascular clamps were applied across both renal pedicles for 15 minutes. Immediately after complete visual reflow of both kidneys, a volume of 100  $\mu$ l of cell suspension that contained  $10^5$  MKPC cells in PBS was injected slowly and directly into the renal parenchyma of each kidney. As controls, 36 mice ( $n = 6$  for each time point in each group) were subjected to an identical protocol of ischemia reperfusion injury but received 100  $\mu$ l of PBS or  $10^5$  NIH3T3 cells of the same volume as MKPC in each kidney. Renal function was assessed by serial measurement of blood urea nitrogen (BUN) by quantitative colorimetric assay kit (Sigma). Mice were sacrificed after 2, 4, and 7 days, and both kidneys were obtained and processed for formalin fixation followed by paraffin embedding or frozen section. Sections were stained with hematoxylin-eosin and examined histologically for the morphologic

changes resulting from ischemic injury. A grading scale (scores of 0–4) for assessment of necrotic injury to the proximal tubules, as outlined by Jablonski et al. [26], was used for the histopathological assessment of ischemia-reperfusion (IR)-induced damage. To study the effect of MKPC on survival, 36 ischemic mice were given PBS and 12 ischemic mice were injected with MKPC.

Data are expressed as mean  $\pm$  SD. Comparisons between groups are evaluated by nonparametric test. A  $p$  value of less than 0.05 denotes the presence of a statistically significant difference.

### Immunohistochemistry

Fixed mouse kidney sections were deparaffinized in xylene and rehydrated through a graded ethanol series to water. After being blocked with 10% normal horse serum in PBS, the slides were stained with primary antibodies overnight at 4°C, biotinylated secondary antibody for 30 minutes, and diaminobenzidine reagent (Vector Laboratories, Burlingame, CA, <http://www.vectorlabs.com>) for 5 minutes. Primary antibodies used were mouse monoclonal anti-E-cadherin antibody (BD, 1:400), rabbit polyclonal anti-Tamm-Horsfall glycoprotein (Santa Cruz, 1:400), mouse monoclonal anti-Ki67 (Upstate, Charlottesville, VA, <http://www.upstate.com>, 1:200), mouse monoclonal anti-GFP (Santa Cruz, 1:1000), rat monoclonal anti-CD34 (Abcam, Cambridge, U.K., <http://www.abcam.com>, 1:500), and rabbit polyclonal anti-Oct4 (Santa Cruz, 1:400).

## RESULTS

### Generation of Myh9 Targeted Mutant Mice and Expression of GFP

We first created *Myh9* targeted mutant mice. The targeted strategy and genotype analysis are summarized in Figure 1A–1C and described in Materials and Methods in detail. In adult *Myh9* targeted mutant mice, GFP is expressed in the glomeruli, interstitium including peritubular vessels, faintly expressed in brush border of the proximal tubules, distal tubules, and collecting ducts (Fig. 1D–1K).

### Isolation of Fluorescent MKPC

To isolate MKPC, we prepared dispersed cells from *Myh9* targeted mutant mice. Cell preparations from C57BL/6 mice were used to determine the level of autofluorescence. The cells prepared from *Myh9* targeted mutant mouse that express GFP 10-fold higher than those from C57BL/6 mouse were sorted (Fig. 2A). After sorting, GFP-positive cells were cultured.

After 8 weeks of culture, most of the GFP-sorted cell types died out and the cultures became monomorphic with spindle-shaped cells (Fig. 2B). These cells contained large nucleus and expressed fluorescence at different passages (Fig. 2B). Some clones have been cultured for more than 100 passages over 1 year without evidence of senescence. MKPC was cytogenetically analyzed at passages 34 and 81. A total of 67 and 74 metaphase spreads were analyzed and counted for each passage. At passage 34, all cells had a normal  $2n = 40$  chromosome complement. The karyological analysis of the MKPC at passage 81 showed that 83% of the metaphases had  $2n = 40$  chromosome (Fig. 2C), 15% of the metaphases had a hypoeuploid chromosome complement ( $2n \leq 39$ ), and 2% of the metaphases had a chromosome number ranging from  $2n = 41$  to  $2n = 79$ . MKPC between 10–20 passages were used in the study.

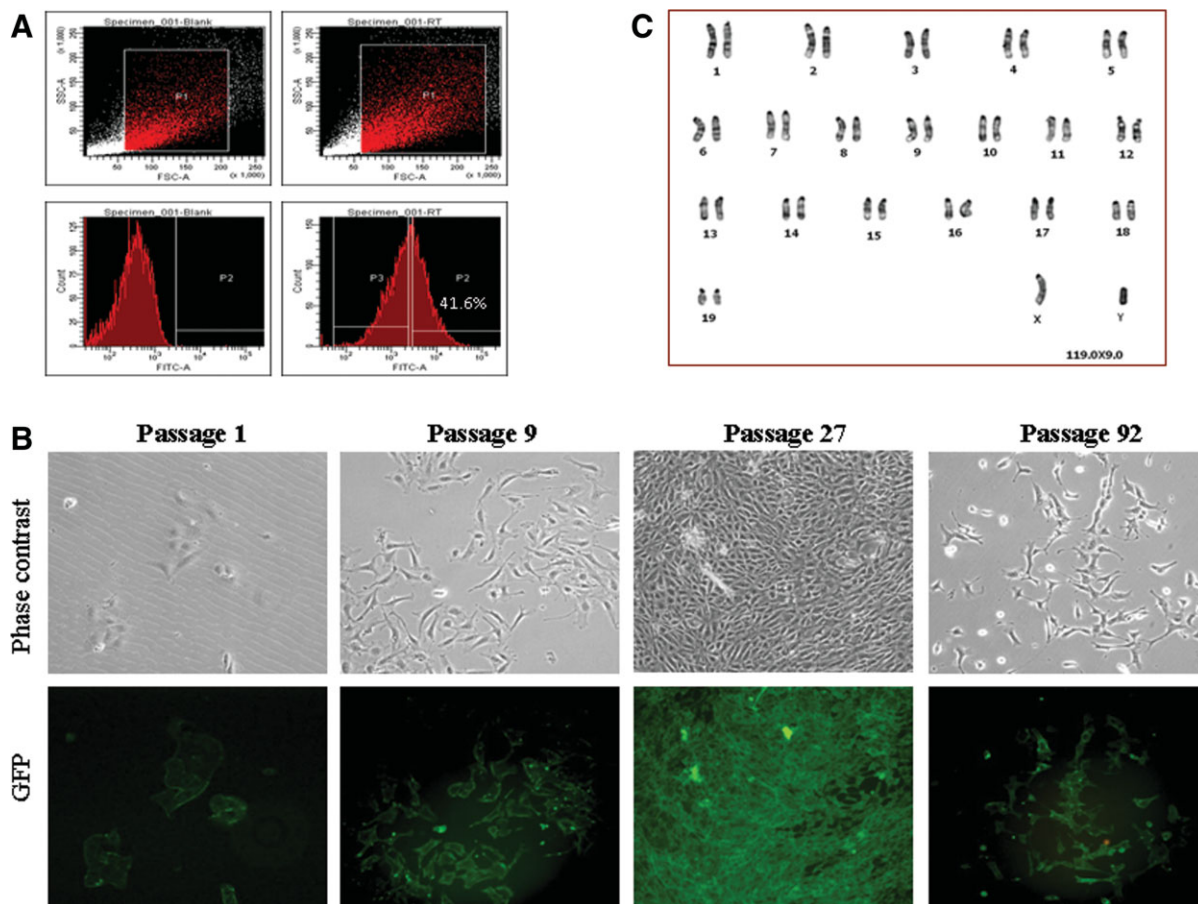


**Figure 2.** Identification of mouse kidney progenitor cells (MKPC) in adult mouse kidney. (A): Flow analyses of kidney cells from adult C57BL/6J mouse (left panels) and *Myh9* targeted mutant mouse (right panels) are shown as representative forward and side scatter plots. Boxed cells in P1 of upper panels represent the lymphogate in C57BL/6J and *Myh9* targeted mutant mice. Cells from *Myh9* targeted mutant mouse expressing green fluorescence 10-fold higher than those from C57BL/6J mouse were sorted (P2 in right lower panel). (B): Morphology of the cells after 1 passage (3 days), 9 passages, 27 passages, and 92 passages after sorting are shown by phase-contrast microscopy and immunofluorescence microscopy. After 9 passages, the cells are monomorphic with a spindle-shaped morphology, contain scant cytoplasm, and maintain fluorescence. MKPC cultured to confluence at passage 27 do not overlay and maintain fluorescence. (C): MKPC have a normal karyotype by cytogenetic analysis. Abbreviations: GFP, green fluorescence protein.

### MKPC Express Renal Progenitor Cell Markers

By immunohistochemistry, MKPC expressed Pax-2, Oct-4, vimentin,  $\alpha$ -smooth muscle actin, CD29, and S100A4 (Fig. 3A) but not SSEA-1, c-kit, E-cadherin, and vWF (Fig. 4). To exclude the possibility that the isolated MKPC are mesenchymal stem cells (MSC), we isolated MSC from the bone marrow of C57BL/6 mice (mMSC) and compared the different phenotypes between MKPC and mMSC. The characteristics of mMSC [27] are confirmed by the expression markers (Fig. 3B) and its ability of differentiation into osteoblasts and adipocytes in vitro (data not shown). As assessed by RT-PCR, MKPC expressed many markers of renal progenitors including Oct-4, Pax-2, Wnt-4, and WT-1, which are expressed in the renal progenitors of metanephric mesenchyme during embryonic development [28], but not CD-34 and Sca-1 (Fig. 3B). MKPC also expressed Rex-1, a target gene of Oct-4. In contrast, MSC did not express these renal markers. These results indicate that MKPC are not MSC. Moreover, we have assessed telomerase activity of MKPC by Telomerase PCR ELISA assay (Roche). In this assay, telomerase transfected mesenchymal stem cells (UE7T) and breast cancer cell line (MCF7) were used as

positive controls. As shown in Figure 3C, MKPC at passages 21, 43, and 83 all exhibit low but detectable telomerase activity. This result is compatible with previous reports showing that adult tissue-specific stem cells have relatively lower telomerase activity than those of embryonic stem cells and cancer cells [29, 30]. Taken together, MKPC are kidney progenitor cells.

### Differentiation of MKPC into Endothelial, Osteoblastic, and Tubular Epithelial Lineages

To further determine the potency of MKPC, we tested their capacity of differentiation in vitro and in vivo. When treated with osteogenic differentiation medium, some population of cells (40% per plate) showed the presence of osteoblasts and stained positive with Alizarin red, indicating osteogenic differentiation (Fig. 4A). Culturing MKPC in matrigel resulted in endothelial morphology with positive staining for von Willebrand factor (Fig. 4B). However, MKPC could not be induced into adipocytes when incubated with adipocyte differentiation medium.

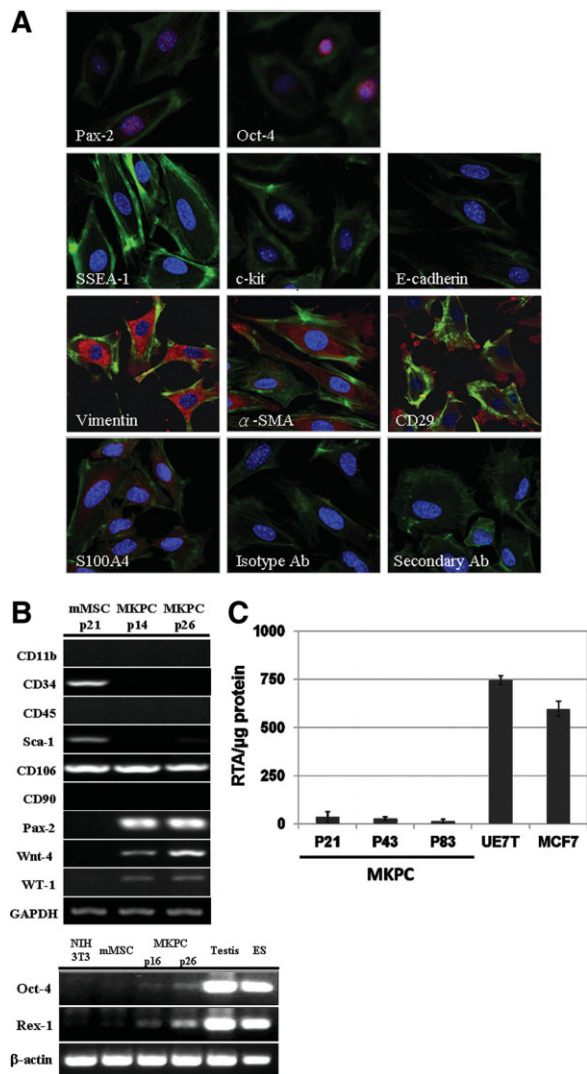


**Figure 3.** Characteristics of MKPC. (A): Confocal immunofluorescence microscopy of fluorescent MKPC (in green) stained with the following antibodies (in red): an anti-Pax 2 antibody, an anti-Oct-4 antibody, an anti-SSEA-1 antibody, an anti-c-kit antibody, an anti-E-cadherin antibody, an anti-vimentin antibody, an anti-alpha smooth muscle actin antibody ( $\alpha$ -SMA), an anti-CD29 antibody, anti-S100A4 antibody, an isotype antibody, and secondary antibody only; MKPC are Pax-2, Oct-4, vimentin,  $\alpha$ -smooth muscle actin, CD29, and S100A4 positive and SSEA-1, c-kit, E-cadherin negative. Scale bars: 20  $\mu$ m. (B): Summary of gene expression on mesenchymal stem cells of the bone marrow from the C57BL/6 mice (mMSC) and MKPC. RNA was extracted and reverse transcribed from mMSC (passage 21) and MKPC (passages 14, 16, and 26). As assessed by reverse transcription polymerase chain reaction, mMSC were characterized by positive expression of CD34, Sca-1, and CD106 and negative expression of CD11b, CD45, and CD90. MKPC were only positive for CD106 and were not MSC. In addition to Pax-2 and Oct-4, MKPC also expressed Wnt-4, WT-1 and Rex-1. Testis and embryonic stem (ES) cells were used as positive control for Oct-4, and NIH3T3 fibroblasts were used as negative control for Oct-4. GAPDH and  $\beta$ -actin were used as internal control. (C): Quantitation of telomerase activity with cell extracts. Relative telomerase activity was determined by Telomerase PCR ELISA. Absorbance was measured at 450 nm and was expressed as the maximum absorbance per  $\mu$ g of protein. UE7T and MCF7 were used as positive controls. UE7T are human bone marrow-derived mesenchymal stem cells that were infected with recombinant retroviruses expressing hTERT, and MCF7 is breast cancer cell line. MKPC exhibit detectable telomerase activity at different passages. Abbreviations: MKPC, mouse kidney progenitor cells.

To examine the *in vivo* differentiation of MKPC, we injected MKPC into the medulla of normal C57BL/6 mice and evaluated for the presence of GFP-positive cells. This was done 30 days after the initial injection to eliminate transient engraftment of cells. Some GFP-positive cells formed vessels with red blood cells (RBC) inside (Fig. 4C). This indicated that endothelial differentiated cells from MKPC organized into functional vessels, connected with the host mouse vasculature. As demonstrated in Figure 4D, some MKPC became lodged in the glomerular capillaries and incorporated into capillaries throughout the cortex and medulla (Fig. 4D–4F). Thirty days after the injection, some MKPC incorporated into distal tubules in the cortex near glomerulus (Fig. 4G, 4H) and some further entered into Henle's loop by expressing Tamm-Horsfall glycoprotein in the medulla (Fig. 4I–4L). These *in vivo* and *in vitro* differentiation results imply that the isolated MKPC were pluripotent.

### The Niche of MKPC Is in the Interstitium of Medulla

To confirm the origin of MKPC, we performed immunohistochemical analyses of Oct-4 in normal kidney of *Myh9* targeted mutant mice. Kidneys of five independent litters of 2- to 12-month-old mice showed similar results, and representative examples are presented in supporting information Figures A and B. Supplemental online Figure A shows sections of different regions of a single kidney co-stained for Oct-4 (brown) and GFP (red). Oct-4 is a POU family transcription factor with limited range of expression confined to embryonic and adult stem cells that controls the differentiation potential of cells [31–34]. There was no Oct-4(+)GFP(+) cell at all in renal cortex (supporting information Figure A, left upper panel). In contrast, significant amounts of Oct-4(+)GFP(+) cells were observed in the medulla and papilla, particularly in areas of the interstitium (supporting information Figure A, right upper and two lower panels). Given that the kidney is rich of vasculature, we examined the relation of Oct-4 positive interstitial cells with endothelial cells. Double immunohistochemical staining of Oct-4 and CD34 showed that Oct-4 positive cells were in close association with endothelial cells (supporting information Figure B). These results indicate that, from medulla to papilla, interstitium is the niche of MKPC.

### MKPC Decreases Infarct Zone and Preserves Renal Function in Mice with Ischemic Renal Injury

If the MKPC were adult kidney stem cells, they might be involved in kidney repair. To determine whether MKPC could affect renal function, we measured BUN levels in mice that had acute renal failure induced by IR injury and received injections of MKPC, 3T3 fibroblasts, or PBS. Immune-deficient SCID mice ( $n = 6$ ) were chosen to escape host immune response of fibroblasts. Cells were filtered and injected into renal parenchyma through the renal pelvis ( $2 \times 10^5$  cell/mouse) immediately after the reperfusion (Fig. 5A). Kidneys treated with MKPC revealed positive GFP immunostaining within the medulla at day 2 and day 4 (Fig. 5B, left and middle panels). To test whether MKPC pertain proliferation potential, BrdU (100 mg/kg) was injected intraperitoneally one day before sacrifice. The results showed that about 20% of GFP positive cells were stained positive for BrdU (Fig. 5B, right panel), providing evidence that MKPC were capable of dividing. Ischemic injury in SCID mice receiving PBS or fibroblasts resulted in significant increases in serum BUN, which peaked at day 2, declined at day 4, and stabilized at day 7. Direct injection of MKPC protected renal function, as reflected by the significantly lower BUN values at day 2 (Fig.

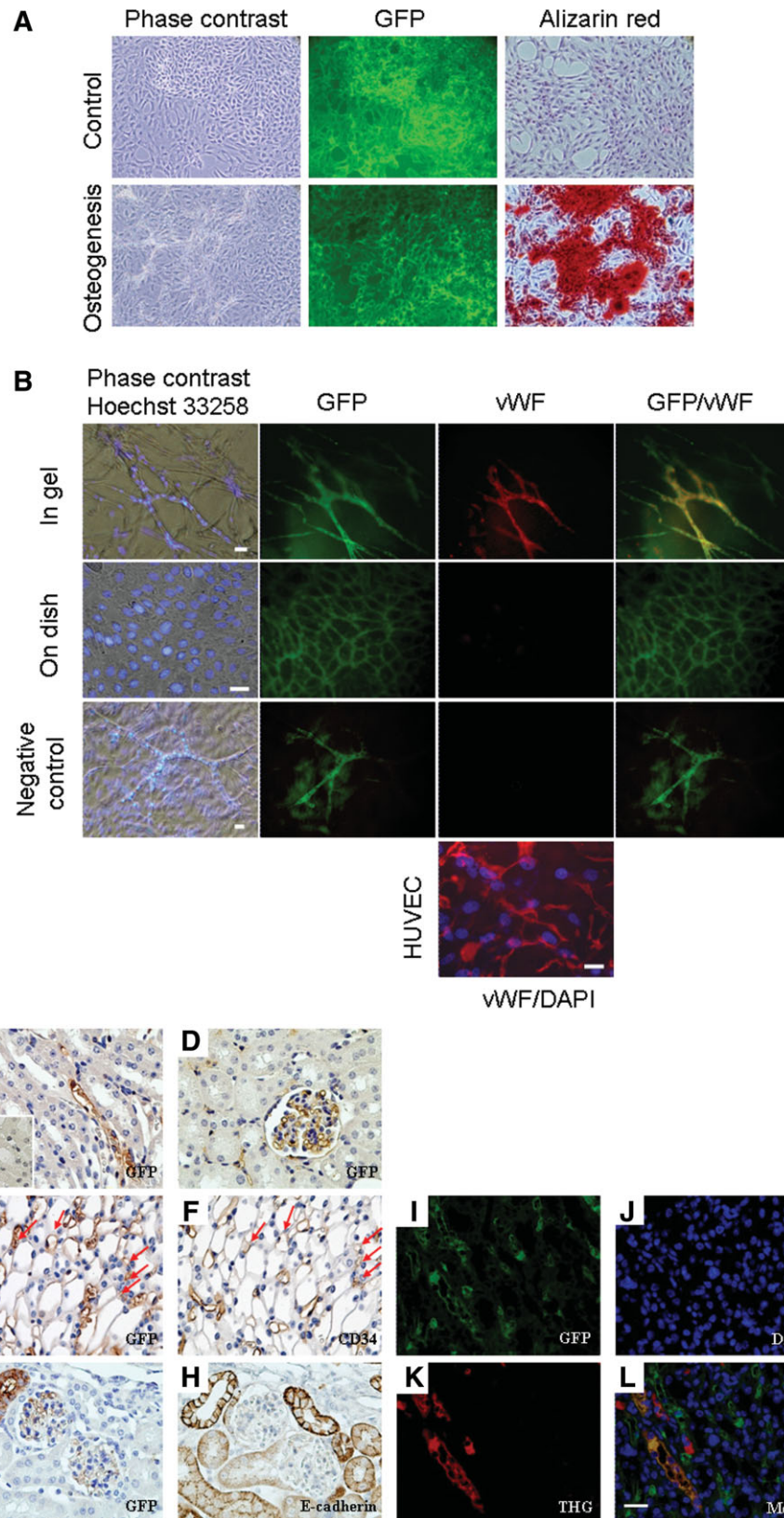


**Figure 4.** MKPC undergo multilineage differentiation. Phase-contrast microscopy and immunofluorescence of MKPC that were incubated under culture conditions that promoted differentiation into osteoblasts and endothelial cells. (A); MKPC that were cultured in the presence of osteogenic differentiation medium developed osteoblastic morphology and were detected by positive staining for calcium deposits using Alizarin red. (B); MKPC that were cultured in matrigel developed endothelial morphology and stained for von Willebrand factor. Differentiated MKPC stained with secondary antibody only were used as negative control. Human umbilical vein endothelial cells cultured on matrigel were used as positive control. (C–L): In vivo differentiation. Immunohistochemistry of the kidney 30 days after injection of MKPC into C57BL/6J mouse. (C): GFP-positive cells formed vessels containing red blood cells. Kidney of C57BL/6J mouse is used as a negative control (inlet). (D): Injected GFP (+) cells lodged in glomerulus and formed capillaries in interstitium. (E, F): The mouse endothelial cells lining the vessels are indicated by positive immunohistochemical staining for GFP (E) and CD34 (F) in consecutive sections in medulla, showing that vessels (arrows) derived from the implanted MKPC. (G, H): Positive tubules demonstrating incorporation of injected MKPC by positive immunohistochemical staining for GFP (G) and E-cadherin (H) in consecutive sections in cortex. (I–L): Immunofluorescence of the kidney. Positive tubules showed incorporation of injected cells (I, in green) and were stained with the Henle’s loop marker Tamm-Horsfall glycoprotein (THG, K in red); nuclei are stained blue. Scale bars: 50  $\mu$ m. Abbreviations: GFP, green fluorescence protein; MKPC, mouse kidney progenitor cells; vWF, von Willebrand factor.

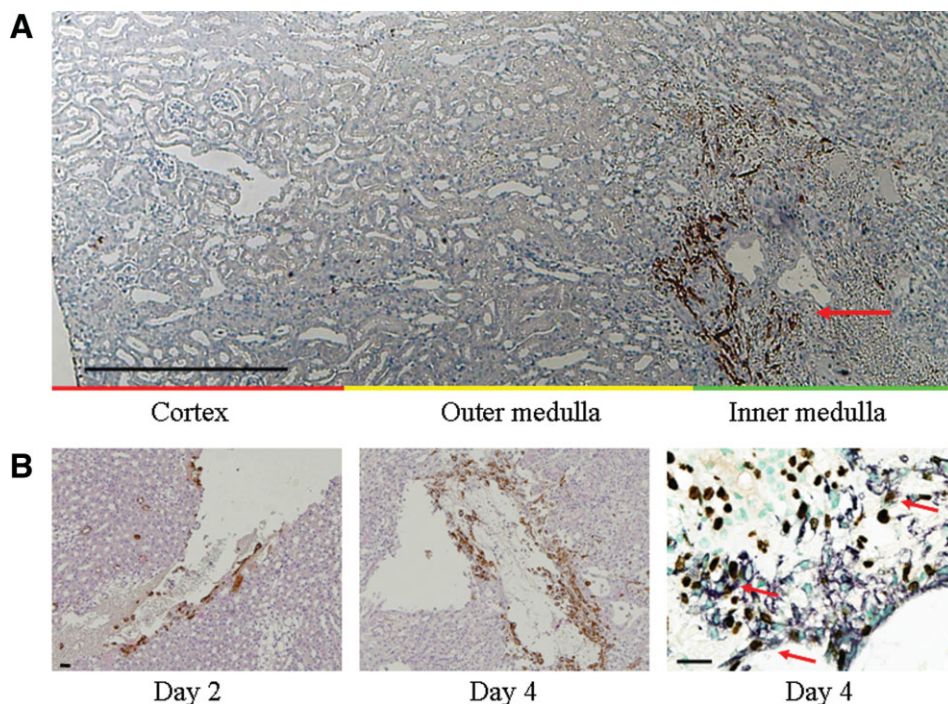


**Figure 5.** MKPC transplantation into the peri-ischemic region proliferate following renal ischemic injury. (A): Immunohistochemistry of the ischemic kidney 4 days after injection of MKPC into renal medulla showing GFP-positive cells at the site of injection. The injection of MKPC is at the inner medulla (arrow). The cortex and outer medulla are the areas of ischemic damage. Scale bar: 1 mm. (B): The numbers of MKPC increase 4 days after injection (vs. 2 days). Co-expression of GFP (in purple, right panel) and BrdU (in brown) in the kidney 4 days after injection of MKPC into the renal parenchyma by double immunohistochemistry, providing evidence that injected cells were capable of dividing. Nuclei are stained green. Scale bars: 50  $\mu$ m. Abbreviations: MKPC, mouse kidney progenitor cells.

6A) in comparison with the PBS- and 3T3-treated mice. It is worth noting that mice treated with MKPC but not fibroblasts displayed a decrease in infarct zone of injured kidney (Fig. 6B).

This improvement of renal function by MKPC treatment was also associated with a better preservation of renal structure (Fig. 6C–6I). Kidneys treated with PBS were characterized by extensive tubular necrosis and more capillary congestion (Fig. 6D) at day 2 and tubular swelling and obstruction with cellular debris (Fig. 6F) at day 4; and at day 7 tubules were still covered with regenerating cells with vacuoles (Fig. 6H). In contrast, kidneys treated with MKPC showed markedly reduced histological features of necrotic injury after ischemia (Fig. 6E, 6G). By day 7, the majority of necrotic tubules disappeared and tubules were almost covered with regenerating cells with brush border (Fig. 6I). Quantitative assessment of renal tubular necrosis using the grading scores of Jablonski et al. [26] is shown in Figure 6J. Histological grading at 2 days after renal ischemia in PBS-treated mice resulted in severe acute tubular necrosis (grade of  $3.2 \pm 0.3$ ,  $n = 6$ ) as compared to that of MKPC-treated mice (grade of  $1.5 \pm 0.3$ ,  $n = 6$ ,  $p < .05$ ).

### Transplanted MKPC Differentiated into Endothelial Cells and Tubular Cells After Ischemic Injury

If MKPC participate in renal repair, these cells or their progeny might be capable of migrating toward and incorporating into other parts of the kidney. To test this hypothesis, we traced MKPC by staining GFP in SCID mice seven days after ischemic injury. As shown in Figure 7A, MKPC were observed mainly in the medulla, in which groups of cells frequently concentrated into a self-limiting nodule around the injection site (Fig. 7B). As shown in Figure 7C–7J, when MKPC were injected after ischemic injury, they differentiated into not only renal tubules but also capillaries. Evidence for the incorporation of injected MKPC into renal tubules was seen mainly in the cortico-medullary junction and the outer

medulla (Fig. 7E–7J). In some areas, all cells in the tubule were GFP positive, whereas in other areas only some cells were positive. After incorporation into the renal tubules, the injected MKPC could express the loop of Henle marker Tamm-Horsfall protein (Fig. 7J). In addition, MKPC also differentiated into capillaries, frequently in groups, which possessed RBC inside (Fig. 7C, 7D).

### MKPC Ameliorates Mortality of Mice with Acute Kidney Injury

We further tested whether MKPC treatment could affect survival, the critical outcome in acute kidney injury. Survival curves of SCID mice with acute kidney injury given PBS or MKPC are shown in Figure 7K. Mice injected immediately after ischemic injury with MKPC survived significantly longer than PBS-treated mice ( $p = .0002$ ). At day 4, only one mouse (8%) injected with MKPC died, whereas 63% of mice died in the PBS group. At day 7, the percentage of surviving mice given MKPC remained at 92%; on the other hand, only 25% of mice given PBS survived at the same time. These results indicate that MKPC not only rescue renal injury but also prolong survival in mice after ischemic damage.

## DISCUSSION

Clinically, after acute kidney injury, the lack of effective treatment leads to potentially catastrophic outcome. Here we examined the positive impact of kidney progenitor cells on the renal outcome after acute ischemic injury. Mice died of uremia after severe tubular necrosis. The treatment using mouse kidney progenitor cells saved lives by improving renal function. Intrarenal injection of mouse kidney progenitor cells protected mice from renal function impairment and consequent death primarily by exerting protective actions against tubular cell damage after ischemic injury.

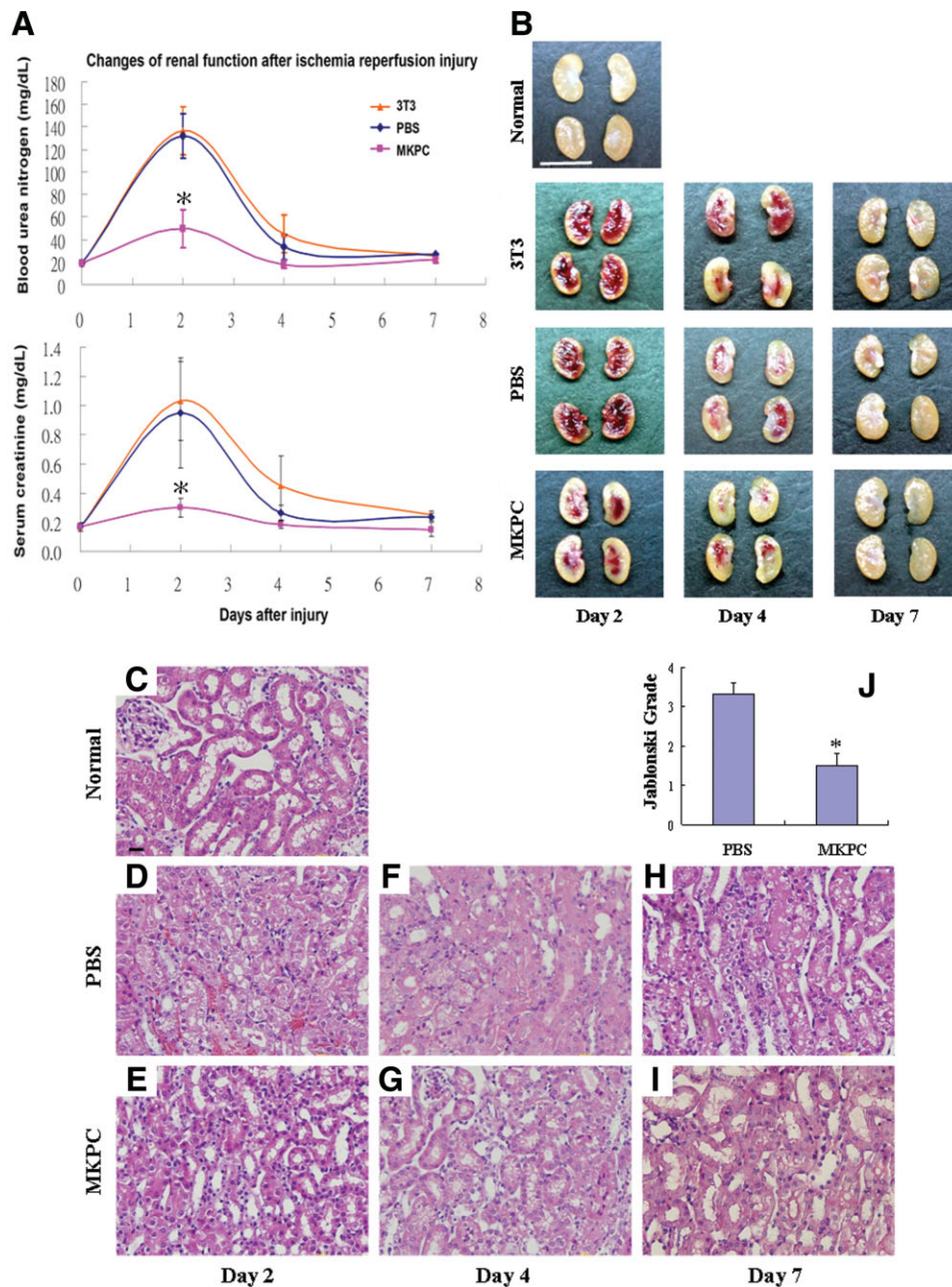


**Figure 6.** MKPC, but not fibroblasts, protect ischemia-reperfusion injured mice from renal function and structure deterioration. (A): Serial blood urea nitrogen and creatinine levels as measured in ischemia-reperfusion injured mice ( $n = 6$  in each group) that received 3T3 fibroblasts ( $\blacktriangle$ ), PBS ( $\blacklozenge$ ), or MKPC ( $\blacksquare$ ). MKPC administration immediately after reflow to mice with acute ischemic injury significantly improves renal function on 2 days after clamping, whereas PBS- and fibroblast-treated mice show no such response. \*,  $p < .02$  MKPC- versus PBS- and 3T3-treated mice. (B): Representative gross morphologies of hemisected kidneys that were untreated (normal) or treated with fibroblasts (3T3, upper panel), with PBS (middle panel), or with MKPC (lower panel) 2, 4, and 7 days after ischemia-reperfusion injury in SCID mice. The infarct zones (dark red areas) are similar in 3T3- and PBS-treated mice but decrease in MKPC-treated mice at each time point. Scale bar: 10 mm. (C–I): Representative photomicrographs of hematoxylin and eosin stained kidney section before induction (C), 2 days (D, E), 4 days (F, G), and 7 days (H, I) of acute renal failure in mice treated with PBS (upper panel) or MKPC (lower panel). There was extensive tubular necrosis and more capillary congestion in the PBS group (D) than in the MKPC group (E). Tubular swelling and obstruction with cellular debris appeared more obvious in the PBS group (F) than in the MKPC group (G) 4 days after injury. By day 7, the majority of necrotic tubules disappeared and tubules were almost covered with regenerating cells with brush border in the MKPC group (I) but with vacuoles in the PBS group (H). Scale bar: 50  $\mu$ m. (J): Jablonski grading scale of histological appearance of acute tubular necrosis from mice subjected to renal ischemia treated with PBS or MKPC. \*,  $p < .05$  MKPC-treated versus PBS-treated group. Data are presented as means  $\pm$  SD. Abbreviations: MKPC, mouse kidney progenitor cells; PBS, phosphate-buffered saline.

The mechanism of how the injected MKPC ameliorated renal function is intriguing with a number of potential possibilities. Indeed, after ischemic injury and intrarenal injection, the engraftment of MKPC into tubular cells was found to be

localized in limited areas rather than diffused widely; the direct contribution of MKPC to tubular repair could be minor as compared to that from the proliferation of the surviving tubular cells. Alternately, our injected cells formed nested

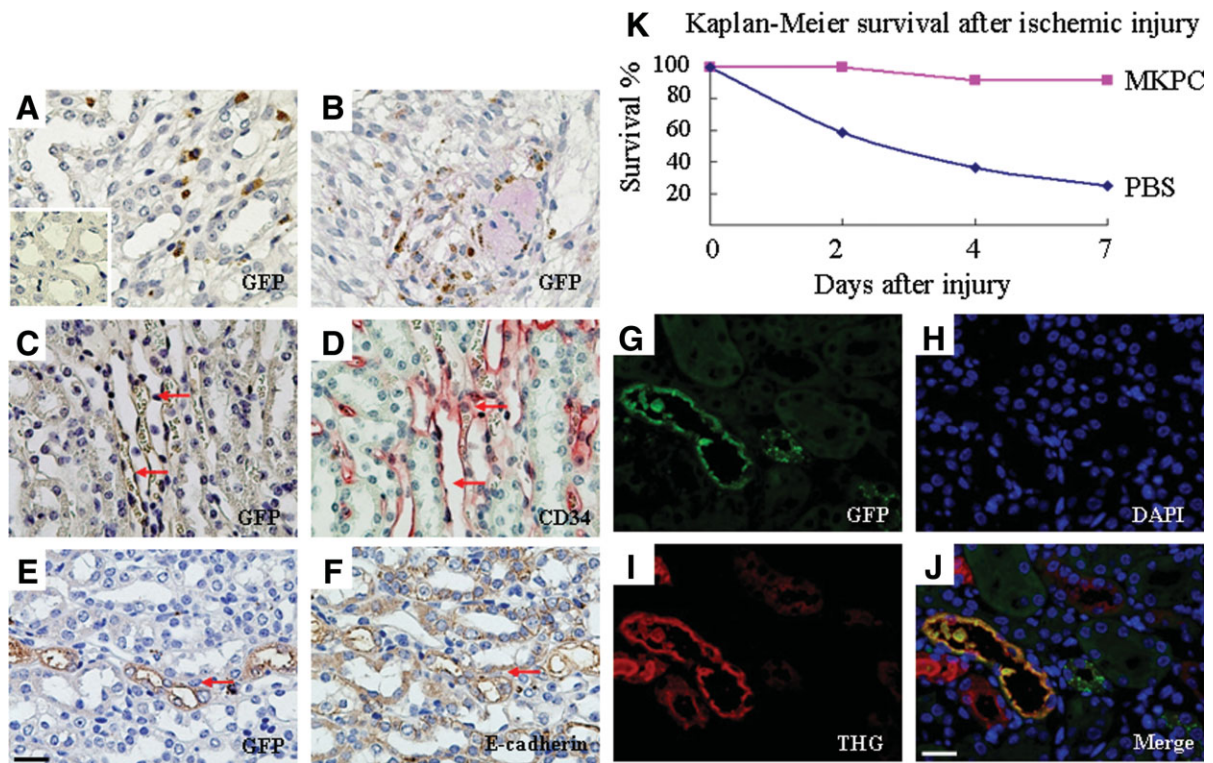


**Figure 7.** MKPC contribute to kidney repair and prolong survival in mice after ischemic injury. (A–J): Kidneys of SCID mice 7 days after ischemic injury and injection of MKPC. Some of the injected MKPC were located in the interstitium (A) and groups of cells concentrated into a nodule-like structure in the medulla (B) detected by immunohistochemical staining of GFP. Kidney of normal SCID mouse is used as a negative control (inlet, in A). (C–F): Expression of GFP, CD34, and E-cadherin in consecutive sections of the kidney. Some GFP-positive cells formed vessel (arrow, in C and D) and incorporated into tubules (arrow, in E and F). (G–J): Immunofluorescence of the kidney section stained with Henle’s loop marker Tamm-Horsfall glycoprotein demonstrating positive (red) staining in GFP-positive cells; nuclei are stained blue. Some individual GFP-positive tubular cells but not Henle’s loop were also found. Scale bar: 50  $\mu$ m. (K): MKPC treatment prolongs survival in mice with acute kidney injury. Kaplan-Meier survival in the MKPC group (■) versus the PBS group (◆). The survival differences between these two groups were tested with the log-rank test that shows a statistical significant difference ( $p = .002$ ). SCID mice given MKPC survived significantly longer than PBS-treated mice. Abbreviations: MKPC, mouse kidney progenitor cells.

capillaries that might be helpful in supplying more oxygen or regenerative materials for kidney repair. In addition to tubular damage, recent evidence has suggested that injury to the renal vasculature may also play an important role in the pathogenesis of ischemic renal injury [35–37]. Following renal ischemia, vasoconstriction or the damaged vasculature may exacerbate hypoxia, prolong the underperfused state of the kidney, and compromise renal function. Targeting this extension phase by treatment with MKPC is thought to provide secondary protection of tubular cells and acceleration of subsequent recovery from acute kidney injury. In addition, it appears that the beneficial effects of MKPC might be mediated through their ability to supply large amounts of angiogenic, anti-apoptotic, and mitogenic factors for epithelial and endothelial cells in kidney repair [38]. Further studies are required to provide insight into the mechanisms. Cell therapy with renal stem cells seems to be a new strategy in the treatment of acute kidney injury. It is obvious that the great therapeutic promise of stem cell therapies makes it mandatory that the mechanisms of action and the long-term safety of this form of therapy are clearly defined.

In the adult kidney, stem cells have been reported to exist in the glomerulus [39], interstitium [11, 13, 40, 41], tubules [10, 12], and papilla [9]. Gupta et al. [12] have isolated a population of renal progenitor cells expressing Oct-4 from renal tubules. Their immunostaining results show that Oct-4 positive cells are only observed in proximal tubule. We demonstrated that Oct-4 positive cells were present in interstitial area of re-

nal medulla. The discrepancy may be explained by the differences in species and isolation strategy. Gupta et al. isolated renal progenitor cells from rats and cultured these cells on fibronectin-coated flasks without passing through sieves. It is possible that fibronectin may provide favorable condition for progenitor cells from the tubules to grow. Our result is supported by the fact that MKPC possess mesenchymal nature, based on their expression of mesenchymal markers, such as vimentin and  $\alpha$ -smooth muscle actin, but not epithelial markers, such as E-cadherin. Moreover, MKPC do not express markers of hematogenous or endothelial progenitor cells, such as CD45, CD34, and c-kit, which negates against the possibility of extrarenal origin of MKPC. This notion bears similarity to the studies where kidney stem cells, BrdU-retaining slow-cycling cells, are localized to the interstitium of renal papilla [9]. A stem cell niche is a restricted environment where presumably the factors that are needed to control growth and differentiation abound, allowing stem cell protection, self-renewing capacity, and differentiation. Our finding that MKPC are not randomly distributed throughout the kidney, but rather are concentrated around blood vessels, is consistent with the concept that it provides a communicating niche between stem cells and systemic messages from vessels. Similarly, in their niche, neuronal stem cells are located in close proximity to the endothelial cells [42, 43]. Studies of the relationship between mouse embryonic neuronal stem cells and endothelial cells have elucidated that endothelial cells not only instruct the neural lineages but also regulate neuronal stem cells proliferation

and induce these stem cells to become neurons in vitro [44]. This evidence strongly suggests that the cellular interactions in the stem cell niche might be an important regulation in the fate of kidney stem cells.

The adult kidney has a low turnover rate under steady-state condition, estimated to be 0.22–0.33%, 0.4%, and 0.45% in tubular epithelial cells, peritubular capillary endothelial cells, and glomerular capillary endothelia, respectively, in the normal human kidney [45]. It suggests that there is a cellular source for kidney maintenance. Unlike regeneration after injury, tubular cell dedifferentiate, re-enter into the cell cycle, and initiate epithelial-to-mesenchymal transition, which is not observed under normal condition. In our study, MKPC differentiated into capillary from cortex to medulla and tubules in normal C57BL/6 mice. The results suggest that kidney stem cells could be one of the sources in the maintenance of cell turnover in normal kidney.

### CONCLUSION

In this study, we have isolated a unique population of cells from adult mouse kidney mesenchyme, MKPC, that exhibit

characteristics of stem/progenitor cells. These cells rescue renal damage and prolong the survival in mice after acute kidney injury. This study opens a new window of cell therapy in acute kidney injury.

### ACKNOWLEDGMENTS

We are grateful to Dr. Norimoto Yanagawa for helpful discussions on this study and critical comments on the manuscript. We also thank Hui-Chuan Cheng, Kuei-Fang Chiang, and Dr. Shiaw-Min Hwang for technical assistance. This work was supported by grants from Kaohsiung Veterans General Hospital (VGHKS96-21, VGHKS97-28, and VGHKS98-26) and the National Science Council (NSC 97-2314-B-075B-005) to P.-T.L.

### DISCLOSURE OF POTENTIAL CONFLICTS OF INTEREST

The authors indicate no potential conflicts of interest.

### REFERENCES

- Morgera S, Schneider M, Neumayer HH. Long-term outcomes after acute kidney injury. *Crit Care Med* 2008;36:S193–S197.
- Schiffli H. Renal recovery from acute tubular necrosis requiring renal replacement therapy: A prospective study in critically ill patients. *Nephrol Dial Transplant* 2006;21:1248–1252.
- Morgera S, Kraft AK, Siebert G et al. Long-term outcomes in acute renal failure patients treated with continuous renal replacement therapies. *Am J Kidney Dis* 2002;40:275–279.
- Jones CH, Jones CH, Richardson D et al. Continuous venovenous highflux dialysis in multiorgan failure: A 5-year single-center experience. *Am J Kidney Dis* 1998;31:227–233.
- Bi B, Schmitt R, Israilova M et al. Stromal cells protect against acute tubular injury via an endocrine effect. *J Am Soc Nephrol* 2007;18:2486–2496.
- Morigi M, Introna M, Imberti B et al. Human bone marrow mesenchymal stem cells accelerate recovery of acute renal injury and prolong survival in mice. *Stem Cells* 2008;26:2075–2082.
- Alexandre CS, Volpini RA, Shimizu MH et al. Lineage-negative bone marrow cells protect against chronic renal failure. *Stem Cells* 2009;27:682–692.
- Bruno S, Grange C, Dereqibus MC et al. Mesenchymal stem cell-derived microvesicles protect against acute tubular injury. *J Am Soc Nephrol* 2009;20:1053–1067.
- Oliver JA, Maarouf O, Cheema FH et al. The renal papilla is a niche for adult kidney stem cells. *J Clin Invest* 2004;114:795–804.
- Kitamura S, Yamasaki Y, Kinomura M et al. Establishment and characterization of renal progenitor like cells from S3 segment of nephron in rat adult kidney. *FASEB J* 2005;19:1789–1797.
- Bussolati B, Bruno S, Grange C et al. Isolation of renal progenitor cells from adult human kidney. *Am J Pathol* 2005;166:545–555.
- Gupta S, Verfaillie C, Chmielewski D et al. Isolation and characterization of kidney-derived stem cells. *J Am Soc Nephrol* 2006;17:3028–3040.
- Dekel B, Zangi L, Shezen E et al. Isolation and characterization of nontubular sca-1+Lin- multipotent stem/progenitor cells from adult mouse kidney. *J Am Soc Nephrol* 2006;17:3300–3314.
- Lazzeri E, Crescioli C, Ronconi E et al. Regenerative potential of embryonic renal multipotent progenitors in acute renal failure. *J Am Soc Nephrol* 2007;18:3128–3138.
- Hughson M, Farris AB III, Douglas-Denton R et al. Glomerular number and size in autopsy kidneys: The relationship to birth weight. *Kidney Int* 2003;63:2113–2122.
- Keller G, Zimmer G, Mall G et al. Nephron number in patients with primary hypertension. *N Engl J Med* 2003;348:101–108.
- Nyengaard JR, Bendtsen TF. Glomerular number and size in relation to age, kidney weight, and body surface in normal man. *Anat Rec* 1992;232:194–201.
- Bertram JF, Soosaipillai MC, Ricardo SD et al. Total numbers of glomeruli and individual glomerular cell types in the normal rat kidney. *Cell Tissue Res* 1992;270:37–45.
- Dressler GR. The cellular basis of kidney development. *Annu Rev Cell Dev Biol* 2006;22:509–529.
- Herzlinger D, Koseki C, Mikawa T et al. Metanephric mesenchyme contains multipotent cells whose fate is restricted after induction. *Development* 1992;114:565–572.
- Oliver JA, Barasch J, Yang J et al. Metanephric mesenchyme contains embryonic renal stem cells. *Am J Physiol Renal Physiol* 2002;283:F799–F809.
- D'Apolito M, Guarnieri V, Boncristiano M et al. Cloning of the murine non-muscle myosin heavy chain IIA gene ortholog of human MYH9 responsible for May-Hegglin, Sebastian, and Fechtner syndromes. *Gene* 2002;286:215–222.
- Sellers JR. Myosins: A diverse superfamily. *Biochim Biophys Acta* 2000;1496:3–22.
- Arrondel C, Vodovar N, Knebelmann B et al. Expression of the non-muscle myosin heavy chain IIA in the human kidney and screening for MYH9 mutations in Epstein and Fechtner syndromes. *J Am Soc Nephrol* 2002;13:65–74.
- Wu Y, Chen L, Scott PG et al. Mesenchymal Stem Cells Enhance Wound Healing Through Differentiation and Angiogenesis. *Stem Cells* 2007;25:2648–2659.
- Jablonski P, Howden BO, Rae DA et al. An experimental model for assessment of renal recovery from warm ischemia. *Transplantation* 1983;35:198–204.
- Peister A, Mellad JA, Larson BL et al. Adult stem cells from bone marrow (MSCs) isolated from different strains of inbred mice vary in surface epitopes, rates of proliferation, and differentiation potential. *Blood* 2004;103:1662–1668.
- Vigneau C, Polgar K, Striker G et al. Mouse embryonic stem cell-derived embryoid bodies generate progenitors that integrate long term into renal proximal tubules in vivo. *J Am Soc Nephrol* 2007;18:1709–1720.
- Hiyama E, Hiyama K. Telomere and telomerase in stem cells. *Br J Cancer* 2007;96:1020–1024.
- Wright LS, Prowse KR, Wallace K et al. Human progenitor cells isolated from the developing cortex undergo decreased neurogenesis and eventual senescence following expansion in vitro. *Exp Cell Res* 2006;312:2107–2120.
- Jiang Y, Jahagirdar BN, Reinhardt RL et al. Pluripotency of mesenchymal stem cells derived from adult marrow. *Nature* 2002;418:41–49.
- Byrne JA, Simonsson S, Western PS et al. Nuclei of adult mammalian somatic cells are directly reprogrammed to oct-4 stem cell gene expression by amphibian oocytes. *Curr Biol* 2003;13:1206–1213.
- Okuda T, Tagawa K, Qi ML et al. Oct-3/4 repression accelerates differentiation of neural progenitor cells in vitro and in vivo. *Brain Res Mol Brain Res* 2004;132:18–30.

- 34 Tai MH, Chang CC, Olson LK et al. Oct4 expression in adult human stem cells: Evidence in support of the stem cell theory of carcinogenesis. *Carcinogenesis* 2005;26:495–502.
- 35 Brodsky SV, Yamamoto T, Tada T et al. Endothelial dysfunction in ischemic acute renal failure: Rescue by transplanted endothelial cells. *Am J Physiol Renal Physiol* 2002;282:F1140–F1149.
- 36 Sutton TA, Mang HE, Campos SB et al. Injury of the renal microvascular endothelium alters barrier function after ischemia. *Am J Physiol Renal Physiol* 2003;285:F191–F198.
- 37 Basile DP. The endothelial cell in ischemic acute kidney injury: Implications for acute and chronic function. *Kidney Int* 2007;72:151–156.
- 38 Tögel F, Hu Z, Weiss K et al. Administered mesenchymal stem cells protect against ischemic acute renal failure through differentiation-independent mechanisms. *Am J Physiol Renal Physiol* 2005;289:F31–F42.
- 39 Sagrinati C, Netti GS, Mazzinghi B et al. Isolation and characterization of multipotent progenitor cells from the Bowman's capsule of adult human kidneys. *J Am Soc Nephrol* 2006;17:2443–2456.
- 40 Hishikawa K, Marumo T, Miura S et al. Musculin/MyoR is expressed in kidney side population cells and can regulate their function. *J Cell Biol* 2005;169:921–928.
- 41 Chen J, Park HC, Addabbo F et al. Kidney-derived mesenchymal stem cells contribute to vasculogenesis, angiogenesis and endothelial repair. *Kidney Int* 2008;74:879–889.
- 42 Alvarez-Buylla A, Lim DA. For the long run: Maintaining germinal niches in the adult brain. *Neuron* 2004;41:683–686.
- 43 Wurmser AE, Palmer TD, Gage FH. Neuroscience Cellular Interactions In The Stem Cell Niche. *Science* 2004;304:1253–1255.
- 44 Shen Q, Goderie SK, Jin L et al. Endothelial cells stimulate self-renewal and expand neurogenesis of neural stem cells. *Science* 2004;304:1338–1340.
- 45 Nadasdy T, Laszik Z, Blick KE et al. Proliferative activity of intrinsic cell populations in the normal human kidney. *J Am Soc Nephrol* 1994;4:2032–2039.



See [www.StemCells.com](http://www.StemCells.com) for supporting information available online.